Neurocomputing 120 (2013) 365–379

Contents lists available at ScienceDirect

Neurocomputing

journal homepage: www.elsevier.com/locate/neucom

A comparative study on local binary pattern (LBP) based face recognition: LBP histogram versus LBP image

Bo Yang [a,b], Songcan Chen [b,*]

[a] College of Computer Science, Inner Mongolia University, Hohhot 010021, PR China
[b] College of Computer Science and Technology, Nanjing University of Aeronautics & Astronautics, Nanjing 210016, PR China

ARTICLE INFO

Article history:
Received 6 December 2011
Received in revised form
18 October 2012
Accepted 21 October 2012
Available online 3 April 2013

Keywords:
Local binary pattern (LBP)
LBP histogram
LBP code
Face recognition
Texture analysis

ABSTRACT

The spatially **e**nhanced **l**ocal **b**inary **p**attern (LBP) **h**istogram (eLBPH) methodology has attained an established position in the field of face recognition (FR) and derived many face analysis approaches. Their implementations follow a similar procedure: first divide a full facial image into some regions (subimages) and individually extract LBP histogram for each region, then concatenate all these regional histograms into a single (global) histogram for final recognition. It has been reported that eLBPH is more effective than the naïve **h**olistic LBP **h**istogram (hLBPH), while the adoption of **h**olistic LBP **i**mage (hLBPI) in FR is relatively few. So, this paper aims to systematically empirically address these issues: (1) Why the simple hLBPH is hardly adopted in FR? (2) Why eLBPH is more effective than hLBPH for FR? (3) hLBPI enjoys what kind of properties for FR. Concretely, we (1) compare the hLBPHs for large-variational facial images with those for standard texture images, and suggest that the LBP histogram feature generally needs certain preprocessing or post-processing for good FR performances; (2) illuminate the reason that eLBPH is more effective than hLBPH for FR, i.e., the enhanced histogram tends to be uniform (more stable than the holistic histogram) and relatively preserve spatial relations of faces, and show the sensitivity of eLBPH to the division region parameter; (3) we study the properties of hLBPI for FR, i.e., hLBPI faithfully preserves the both spatial structure and intrinsic appearance details of a facial image, inherits the attractive properties of the LBP operator and does not require the calculation of histogram for FR; (4) comprehensively evaluate and compare hLBPI, hLBPH, eLBPH and some subspace algorithms on the benchmark face datasets (*FERET*, *Extended YaleB*, *CMU PIE*, *AR*); (5) conclude that hLBPI, hLBPH and eLBPH respectively are suitable for face representation under what conditions, and expect providing practitioners with guidance in selecting appropriate approaches for real tasks.

1. Introduction

The nonparametric local binary pattern (LBP) operator was first mentioned by Harwood et al. [1] and then introduced to image texture description by Ojala et al. [2] for texture analysis. With the LBP operator, the occurrences of the LBP code for an image are collected into a histogram, which is used in texture classifications by histogram matching methods such as histogram intersection, Chi-square [3,4], etc. The operator enjoys some attractive properties such as tolerance to monotonic gray-scale, illumination variations, and computational simplicity, and has been demonstrated to be highly discriminative [3]. Due to these properties, it considerably successfully is used to textures analysis [5–12]. In order to rather serve to real tasks, the original LBP operator [1,2] with the 3×3 neighborhood is extended to different-size of neighborhoods and uniform pattern versions [3,13].

The LBP operator has recently been used to face description [14–24] by adopting the region-division and concatenation histogram strategy. The spatially enhanced LBP histogram (eLBPH) is the first LBP-based face recognition (FR) approach (eLBPH for short hereafter) [14,15], which divides[1] a full facial image into some regions (subimages), then extracts a regional LBP histogram from each region and finally concatenates all regional histograms into a single global histogram as a face representation for recognition. The eLBPH methodology has permeated into many face analysis domains including face recognition [17–22], facial expression recognition [23,24], gender recognition [25], face detection [26], face authentication [27–29], shape location [30] and so on. Moreover, the boosting extension of eLBPH has also been utilized in the Beijing Olympics 2008 for identifying visitors [31,32]. It has been reported that eLBPH is more effective than the naïve **h**olistic LBP

* Corresponding author. Tel.: +86 25 84892956; fax: +86 25 84892400.
E-mail address: s.chen@nuaa.edu.cn (S. Chen).

[1] The division may be a overlapping (or not) way, the latter is adopted in this paper.

0925-2312/$ - see front matter © 2013 Elsevier B.V. All rights reserved.
http://dx.doi.org/10.1016/j.neucom.2012.10.032

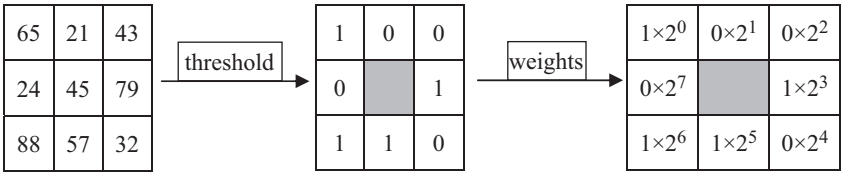

LBP code of the center pixel 45:$1\times2^0+0\times2^1+0\times2^2+1\times2^3+0\times2^4+1\times2^5+1\times2^6+0\times2^7=1+8+32+64=105$

Fig. 1. An example of the original LBP operator.

histogram (hLBPH), while the adoption of **h**olistic LBP **i**mage (hLBPI) in FR is relatively few.

Motivated from different developments and utilizations of the LBP histogram and LBP image features in face recognition, the comparative work systematically empirically addresses these issues:

(1) Why the simple hLBPH is hardly adopted in FR?
(2) Why eLBPH is more effective than hLBPH for FR?
(3) hLBPI enjoys what kind of properties for FR.

More concretely, our insights and contributions mainly involve as follows:

(1) We compare the hLBPHs for large-variational facial images with those for standard texture images (*c.f.* Figs. 4 and 5 in Section 3), and suggest that the hLBPH is not quite appropriate for facial image representation and the LBP histogram feature generally needs certain preprocessing such as region division for good FR performances.
(2) We illuminate the reason that eLBPH is more effective than hLBPH for FR, i.e., the enhanced histogram tends to be uniform (more stable than the holistic histogram) and preserves spatial relations of faces. (*c.f.* Figs. 6–9 in Section 3). Specifically, we illustrate in detail that the spatial relation of eLBPH is relatively rather than absolutely preserved, and show the sensitivity of eLBPH to the division region parameter. (*c.f.* Fig. 6 in Section 3 and Fig. 14 in Section 4). Here it should be pointed out that though the number of sub-blocks per image is studied also in [33], different from it, our purpose is to exhibit the properties of eLBPH as adequately and objectively as possible.
(3) We study the properties of hLBPI for FR via Fig. 10, from which we can observe that hLBPI inherits the attractive properties of the LBP operator [2–4], does not need histogram calculation and region division at all, and quite faithfully preserves both the spatial structures and the intrinsic appearance details of a facial image. Likewise, it should be pointed out that though a few papers were previously proposed for utilization of the hLBPI [34,35] and followed by other papers [16,29] reviewing such utilizations especially for face authentication or verification, relatively less work explores the hLBPI properties itself and suitable tasks for it, let alone the comparative study between the hLBPI and the LBPH (hLBPH and eLBPH) features for the FR. In this paper, we compare the difference between hLBPI and LBPH (hLBPH and eLBPH) features and finally indicate their respective appropriate tasks, so as to provide guides for practitioners. Concretely speaking, on one hand, from (1) above we confirm that the holistic approach is simpler, however, unfortunately, the hLBPH is quite unsatisfactory to facial images and generally needs certain preprocessing such as region division; from (2) above we know that both the locality of region division and spatial preservation of regional histogram concatenation play key roles in eLBPH for FR, however, the eLBPH is more complex and only relatively rather than absolutely preserves spatial relations for a face; from (3) above we verify that the sensitivity for the region parameter is a limitation of eLBPH for effective recognitions. On the other hand, the hLBPI by its definition (in Section 3.3) is the image preprocessed by the LBP operator for an input image, and thus inherits the attractive properties of the LBP operator [2–4], dispenses with histogram calculation and region division at all, and faithfully preserves both the spatial structures and the intrinsic appearance details of a facial image (*c.f.* Fig. 10 in Section 3 and Fig. 14 in Section 4).
(4) We comprehensively evaluate and compare hLBPI, hLBPH, eLBPH and some typical FR approaches based on subspace (Eigenface [36], Laplacianface [37] and Fisherface [38]), as demonstrated in the challenging datasets (Section 4 experiment).
(5) We conclude in some depth the respective properties of hLBPI, hLBPH and eLBPH as well as suitable FR tasks.

Rest of the parts of this paper is organized as follows: Section 2 briefly reviews the LBP operator, its popular extensions and the eLBPH based FR approach. Section 3 addresses the so-raised issues. Section 4 firstly experimentally evaluates and compares the hLBPI, hLBPH, eLBPH and some subspace learning algorithms for FR, and then hLBPI and hLBPH for texture images. Section 5 gives the conclusion remarks to provide guides for practitioners.

2. Related approaches

2.1. Local binary pattern (LBP)

Ojala et al. [2] introduced the LBP texture operator, which originally works with the 3×3 neighborhood. The pixel values of eight neighbors are thresholded by the value of the center pixel, then, the so-thresholded binary values are weighted by powers of two and summed to obtain the LBP code of the center pixel. Fig. 1 shows an example of the LBP operator. In fact, let g_c and $g_0,\ldots, g_7$ denote respectively the gray values of the center and its eight-neighbor pixels, then the LBP code for the center pixel with coordinate (x, y) is calculated by

$$LBP(x,y)=\sum_{p=0}^{7}s(g_c-g_p)2^p \tag{1}$$

where $s(z)$ is the threshold function

$$s(z)=\begin{cases}1, & z\geq0\\ 0, & z<0\end{cases} \tag{2}$$

In traditional real tasks, the statistic representation of LBP codes, LBP histogram (LBPH), usually is used. That is, the LBP codes of all pixels for an input image are collected into a histogram as a texture descriptor, i.e.,

$$LBPH(i)=\sum_{x,y}\delta\{i,LBP(x,y)\},\quad i=0,\ldots,2^7 \tag{3}$$

where $\delta(\cdot)$ is the Kroneck product function.

One extension of the LBP operator is to use neighborhoods of different sizes [3]. The extension is able to take any radius and

neighbors around a center pixel, denoted by $LBP_{P,R}$, by using a circular neighborhood and the bilinear interpolation whenever the sampling point does not fall in the center of a pixel. For example, $LBP_{16,2}$ refers to 16 neighbors in a neighborhood of radius 2. Fig. 2 shows an example with different radii and neighbors.

Another extension is the so-called uniform patterns [3], denoted by $LBP_{P,R}^{u2}$. A LBP binary code is called *uniform* if it contains at most two bitwise transitions from 0 to 1 or vice versa when the binary string is considered as a circular. For example, 00000000, 00011110 and 10000011 are uniform patterns. For the computation of LBPH, the uniform patterns are used such that each uniform pattern has an individual bin and all non-uniform patterns are assigned to a separate bin. So, with 8 neighbors, the numbers of bins for standard LBPH are 256 and 59 for uniform patterns LBPH, respectively; with 16 neighbors, the numbers of bins are 65,536 and 243, respectively. Clearly, the uniform patterns are able to reduce the length of histogram vectors.

2.2. Spatially enhanced local binary pattern histogram (eLBPH) based face recognition (FR)

In LBP based FR approaches, the eLBPH presented by Ahonen et al. [14,15] attains an established position because the following approaches adopt the similar ideas [17–32]. To extract the eLBPH feature of a face, first, a facial image is divided into d regions R0, R1,…, R_{d-1} and each regional LBPH is individually calculated, then these resulting d regional LBPHs are concatenated into a spatially enhanced LBPH (eLBPH) in the same order for all images. The eLBPH feature vector has length of $d \times l$ where l is the length of a regional LBPH. Fig. 3 shows an example of the eLBPH feature, where $d=5\times5=25$ and $l=256$, i.e., the length of eLBPH feature vector is $25\times256=6400$.

After the eLBPH feature vector is extracted, the FR is performed by resorting to the k-nearest-neighbor classifier based on the histogram matching techniques such as the popularly used Chi-square measure

$$d_{\chi^2}(M,S)=\sum_{i=1}^{B}\frac{(M_i-S_i)^2}{M_i+S_i} \tag{4}$$

where M and S are the gallery and probe histogram objects, respectively; B is the number of bins in the histogram.

3. Answers on the so-raised issues

In this section, we detailedly address the so-raised issues. The Brodatz texture [39] and Yale face [40] databases are adopted for illustration. Adoption of Brodatz is attributed to its popularity as a benchmark texture analysis database [1–8], particularly, its texture images are all at the standard position without large brightness changes and the hLBPH is successful on it; at the same time, the facial images in Yale have large variations in expression, illumination and occlusions, which often emerge in real world.

3.1. Why is hLBPH not directly adopted for FR?

As well-known, the simple hLBPH has widely been applied to standard texture analysis [1–9], however, the current researchers does not directly adopts it for FR but appeals to the complex region-division based variant eLBPH [14,15], why is that? In order to more clearly address this issue, we experimentally compare the original input images and LBP histograms of standard textural and facial images, where $LBP_{8,1}$ is adopted. We respectively perform two groups of experiments to show the differences of histogram representation between such two categories of images. In group 1, we compare the differences between different-class standard textural and different-person facial images, as illustrated in Fig. 4; in group 2, we compare the differences between the same-class textural and the same-person facial images, as illustrated in Fig. 5.

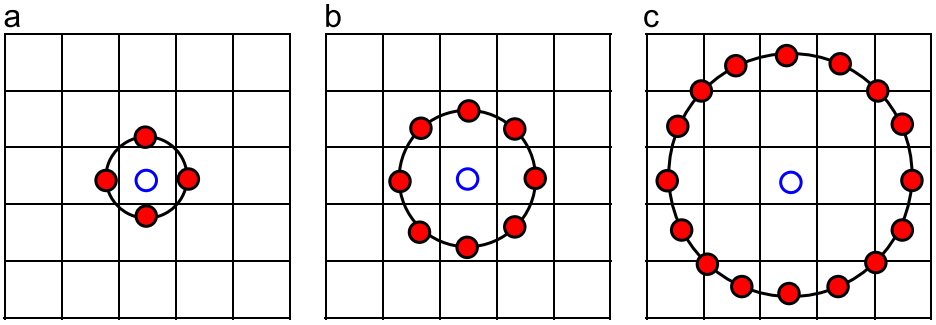

Fig. 2. Circular neighborhoods of the center pixel '○' with different neighbors '●': (a) $LBP_{4,0.5}$, (b) $LBP_{8,1}$, (c) $LBP_{16,2}$. The pixel values are bilinearly interpolated when the sampling point is not in the center of a pixel.

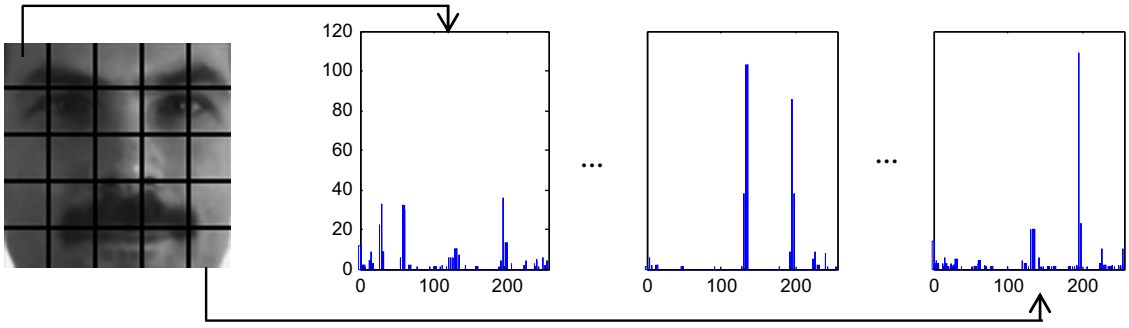

Fig. 3. An example of extracting eLBPH feature vector.

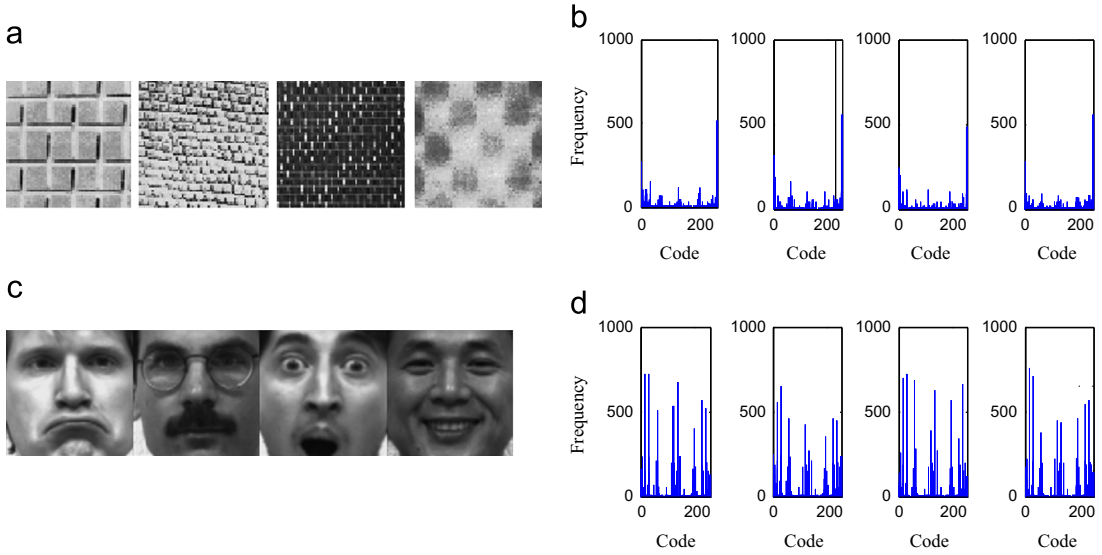

Fig. 4. Input images and LBP histograms for the different-class textural and different-person facial images. (a) texture images, (b) LBP histogram for (a), (c) facial images and (d) LBP histogram for (c).

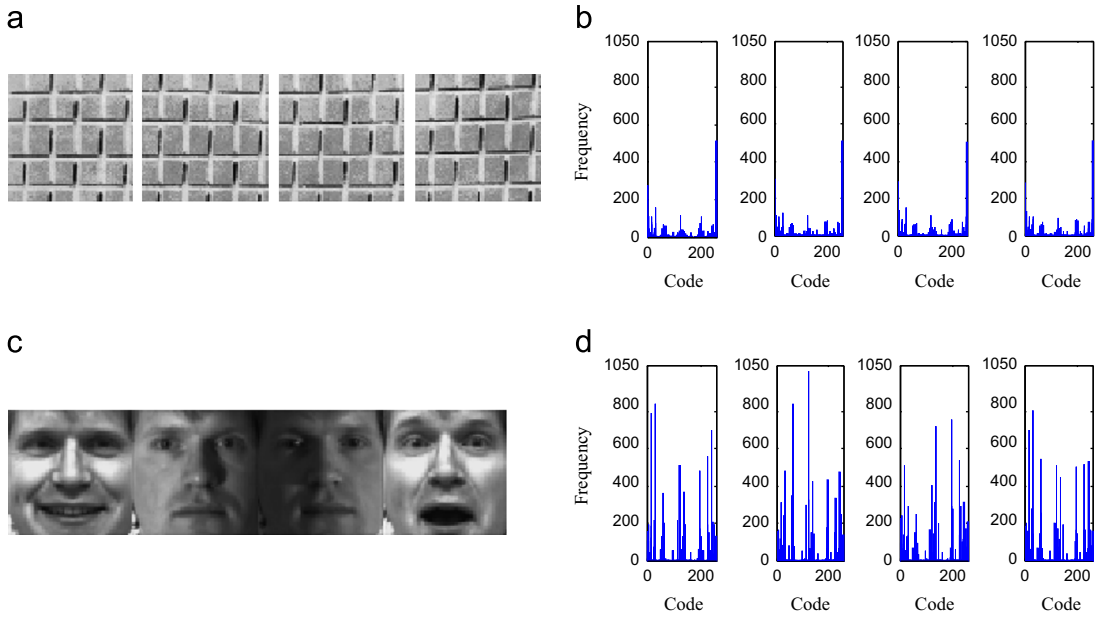

Fig. 5. Input images and LBP histograms for the same-class textural and the same-person facial images. (a) texture images, (b) LBP histogram for (a), (c) facial images and (d) LBP histogram for (c).

By the comparison Fig. 4(a) and (c), it can be clearly seen that the facial appearances are entirely different from the standard textural ones. Specifically, from Fig. 4(a), we can observe that the texture appearances densely cover coarse textures. As defined in [1] "essentially, textures are replications, symmetries, and combinations of various basic patterns or local image functions, usually with some random variation.", and as suggested by Laws [41,42], "many natural and artificial textures are measurably 'loaded' with distributions of various specific local patterns of textures". *In other words, the textures of such images are close to uniform or have certain statistic property*. By contrast, a face in Fig. 4(c) is a dynamic and non-rigid object with various large variations such as illuminations, occlusion, expressions, etc. [17].

Due to the differences between the two categories of images, naturally, the respective LBP histograms are different to great extent, as shown in Fig. 4(b) and (d), respectively. Comparing Fig. 4 (b) with (d), we can find that the LBP histograms for texture images are relatively stable except for the two bins of 0 and 255 whereas very fluctuant for a face, which reflects that the variations are relatively small for standard texture images and the 'spot/flat' texture patterns account for majority while the other texture patterns approximately tend to uniformly distribute, yet considerably large variations for face images and the histograms are very diverse and almost out-of-order.

Figs. 5(a)–(d) shows 4 input images and their corresponding LBP histograms of the same-class textures and the same-person faces, respectively. We find that it is relatively difficult to distinguish the input images (in fact, the space is inserted between texture images) and their corresponding histograms for the same-class textures because the variations within the same-class texture

images are relatively very small; on the contrary, such case does not hold for the same-person face because the variations within the same-person face are relatively very large.

From the above analysis, we have known: one reason behind the success of hLBPH for standard texture images is that the holistic images of standard textures are relatively small variational and thus their corresponding LBP histograms are more stable; whereas hLBPH is not quite favorable for facial images because facial images are often large variational. In fact, the hLBPH is to average overall LBP codes of holistic image area, and thus is a statistic representation of LBP codes. So, if the underlying distributions of textures do not tend to uniform, then the corresponding statistic representation hLBPH would be unreliable. In this sense, it is clear that textures of facial images are not close to uniform due to various variations and thus the hLBPH is not favorable. At the same time, we also know that preprocessing such as region division can mitigate large variations of an input image to certain extent, hence, which indicates the rationality of the eLBPH to certain degree.

It should be pointed out that the examinations on texture and facial images in this subsection are limited to the standard texture and large-variational facial ones. In fact, for non-standard or large-variational texture images, the hLBPH based texture analysis performance often deteriorates dramatically if no preprocessing is made [5,7,43], which supports the undesirability of hLBPH for large-variational images including facial ones; whereas facial images in real-world generally are large variational, even if the standard facial images exist, the variations of their appearances generally are larger than the standard texture ones. Hence, we suggest that the hLBPH is not quite favorable for facial image representations, and the adoption of LBP histogram feature generally needs appeal certain preprocessing such as region division for good FR performances since the variations within subimages are relatively less than the whole facial images.

3.2. Why is eLBPH more effective for FR than hLBPH?

The references [14,15] claimed that the eLBPH approach was motivated by two reasons: (1) "These local features based and hybrid methods seem to be more robust against variations in pose or illumination than holistic methods." (2) "trying to build a holistic description of a face using texture methods is not reasonable,…, for faces, retaining the information about spatial relations is important." Here, we aim to intensively analyze and investigate why eLBPH is more effective than hLBPH for FR.

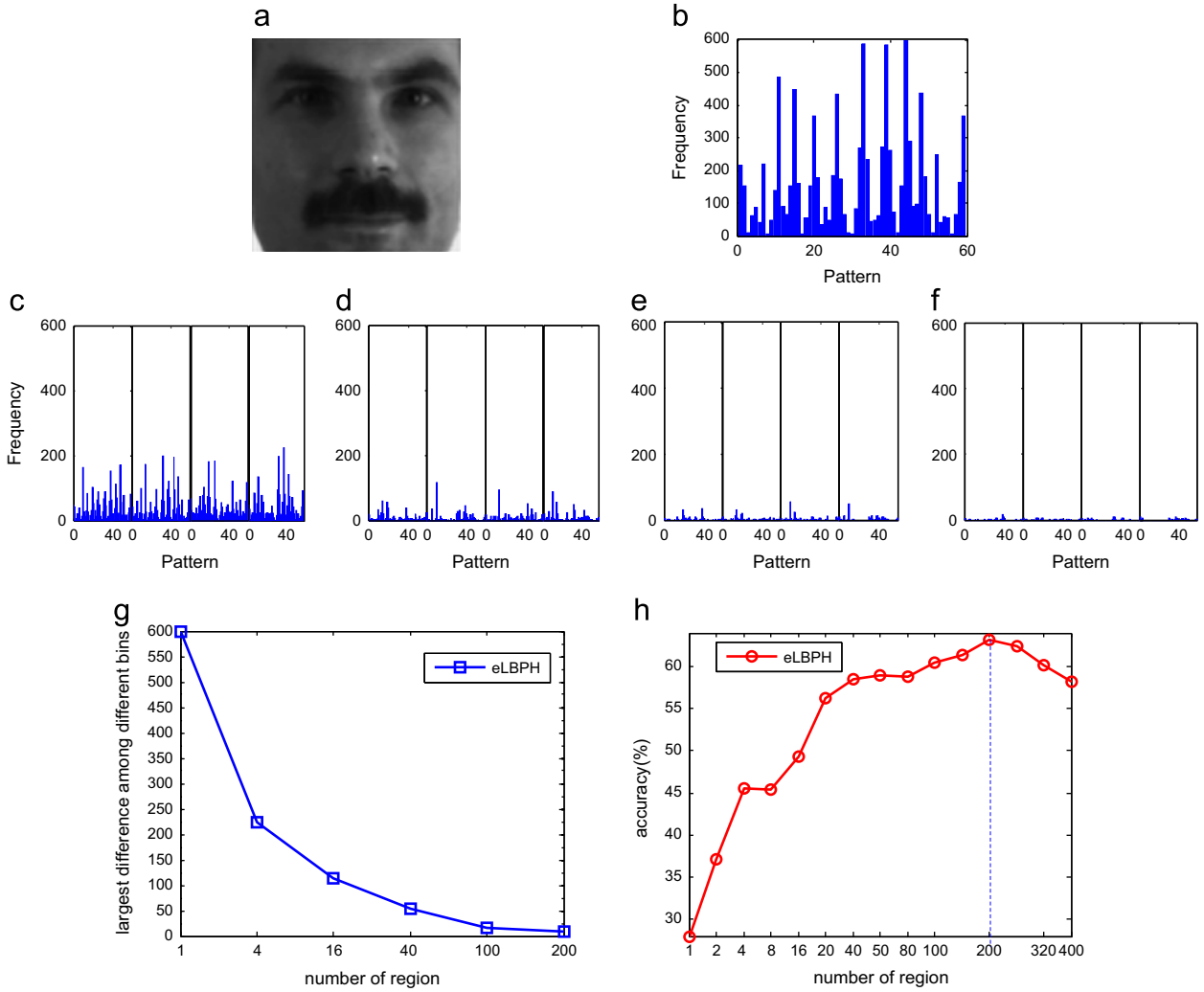

Fig. 6. Example for change of so-divided region number. (a) Input image, (b) the histogram for the whole face (one region), (c) the concatenated histogram for 4 ($=2\times2$) regions, (d)–(f) the first 4 regional histograms of concatenated histogram for 16 ($=4\times4$), 40 ($=4\times10$) and 100 ($=10\times10$) regions, (g) the largest difference among LBP codes vs. number of so-divided region corresponding to (b)–(f) where the largest difference is obtained by the maximum of LBP code subtracting the minimum, (h) accuracy (%) vs. number of so-divided region, with $LBP^{u2}_{8,1}$.

Generally speaking, the eLBPH is more complex than hLBPH, because it nevertheless not only requires region division but also concatenates all region LBP histograms. However, such region division and histogram concatenation make eLBPH more effective than hLBPH for FR, which are detailedly analyzed as follows:

1) As well known, the local feature is more robust against image variations. So, the region division strategy in eLBPH makes each subimage less-variational, as a result, the concatenated LBP histograms are less-fluctuant, more stable, reliable and effective than hLBPH.
   From the analysis in Section 3.1 we have known the largely fluctuant hLBPH is unfavorable for facial images due to large variations of facial images, as shown in Fig. 6(b). By contrast, if the whole face is divided into some regions and one LBP histogram for one region is individually calculated, as shown in Fig. 6(c)–(f), then variations within-region are less than ones of the whole image, in other words, textures within-region relatively tend to uniform, and thus each regional histogram becomes less fluctuant; with the increase of divided regions, each regional histogram gradually becomes more stable, as shown in Fig. 6(g), the largest difference among different bins dramatically drops from 599 for the whole face (one region) to 9 for 200 regions. Hence, the so-concatenated histogram is less-fluctuant and more reliable for facial representation. These results are consistent with the conclusion in Section 3.1 that the less variational an image is, the more reliable the extracted LBP histogram is.
2) With such a region-division and histogram concatenation strategy, the eLBPH preserves the spatial relation for face, as shown in Fig. 7. While the whole face is divided into the left and right regions shown in Fig. 7(a), the spatial relation of left and right parts is basically preserved in the concatenated histogram, as shown in Fig. 7(b); likewise, the whole face is divided into the three regions (the upper, middle and bottom) shown in Fig. 7(c) and the four regions (the left upper, right upper, left bottom and right bottom) shown in Fig. 7(e), the corresponding concatenated histograms shown in Fig. 7(d) and (f) respectively show the spatial preservations of the so-divided region relations for the face.

However, it is necessary to point out that eLBPH only relatively rather than absolutely preserves the spatial relation for face. As illustrated in Fig. 8, the whole face is divided into the left and right regions, the corresponding two regional histograms are concatenated into the eLBPH, which preserves the left and right spatial relations for the face. However, for a region, taking the right region as an example, the LBP codes of "15" are fallen into the same bin while they respectively come from three different locations, i.e., eyebrow, face and cheek. Clearly, within the right region, the spatial relation information is absolutely lost. For the left region (or any region of other division ways), there also exists the same loss of spatial relation. From the relative spatial preservation of eLBPH for face, it is not difficult to conclude that the hLBPH does not preserve any spatial information of face due to its histogram statistic over the whole face.

Moreover, the so-called spatial preservation of eLBPH is closely related to the number of so-divided regions. From Fig. 7 it can be seen that when the whole face is divided into two, three and four regions, the corresponding spatial relations of these so-divided

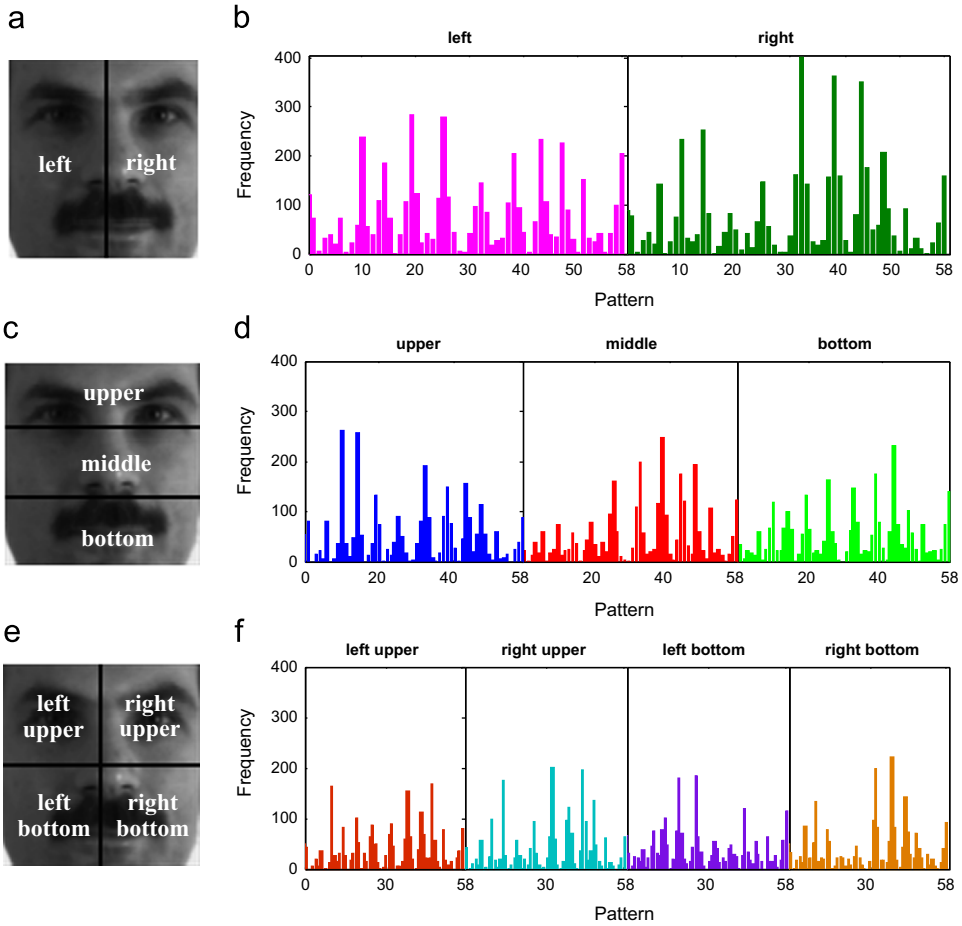

Fig. 7. Example of spatial preservations with different divided regions.

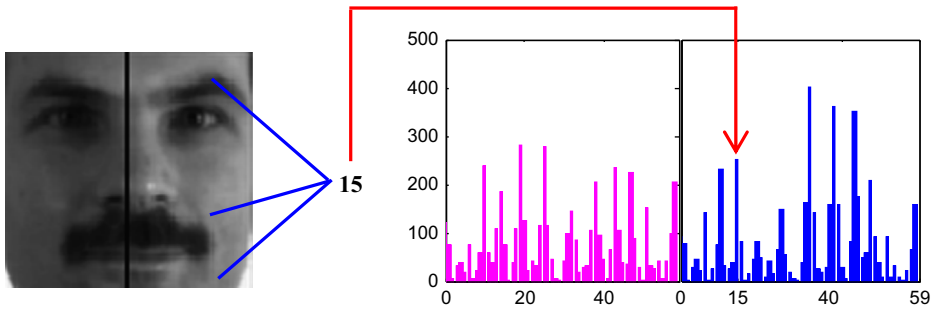

Fig. 8. The equal LBP code values into the same bin from different locations.

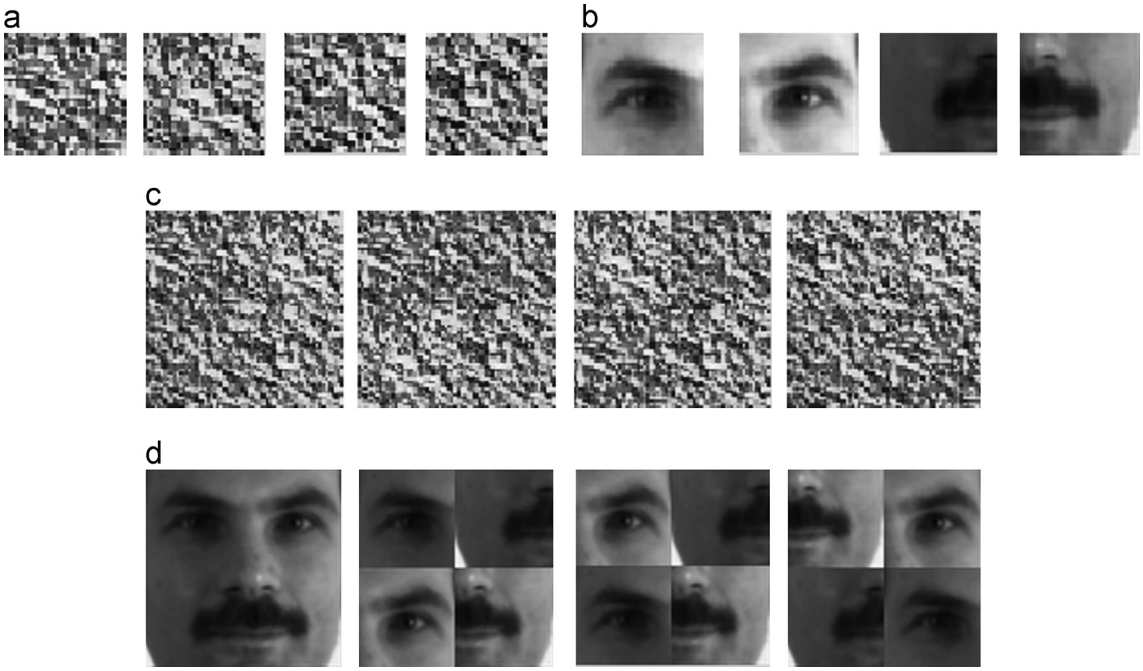

Fig. 9. Subimages of standard textural and facial images and their rearrangements. (a) Subimages of texture image, (b) Subimages of facial image, (c) Four rearrangements of subimages in (a) and (d) Four rearrangements of subimages in (b).

regions are preserved in the concatenated histogram. That is, with the d divided regions, the spatial relations of the d regions for a facial image are rightly preserved in the eLBPH. Therefore, the larger the number of so-divided regions is, the better the spatial relation of face is relatively preserved, and the FR performance also is consequentially increased. However, unfortunately, it is impossible for eLBPH to absolutely preserve such spatial relations, the reason is: for a facial image with 100×100 ($=10{,}000$) size, the absolute spatial preservation requires the number of so-divided regions reaches $d=10{,}000$, i.e., one region per pixel, which is obviously meaningless by the definition of LBP operator, expensive and unreliable as demonstrated in Fig. 6(h) that the recognition performance gradually decreases with the further increase of so-divided region number followed 200.

In fact, by the comparisons standard textural images and facial ones in Section 3.1, it is not difficult to find that the spatial preservation for a facial image is more important than that for a standard textural one. The standard textures tend to uniform and regularly-repeated; if a texture image is divided into some sub-images as shown in Fig. 9(a), then the appearances within-subimage generally are the same as (at least very similar to) the one within whole image, and thus it is relatively difficult to distinguish the various rearrangements shown in Fig. 9(c) of these subimages. However, such a property is not true for a facial image especially for the one with diverse variations, because various subimages of a facial image usually exhibit more likely different appearances as shown in Fig. 9(b), and the unique one of all rearrangements of these subimages, as the first image shown in Fig. 9(d), actually is a face, by contrast, the others are not at all, as the last three rearranged images illustrated in Fig. 9(d). Clearly, the faithful or absolute spatial preservation for a face is favorable for good recognition performance, unfortunately, which is incapable for eLBPH, however, fortunately, actually capable for the forth-coming approach in Section 3.3.

In addition, eLBPH possibly yields a longer feature vector than the input image itself. For example, for an image of size 100×100, the length of feature vector for hLBPH equals to 65,536 with $LBP_{16,1}$; and at the same time, if the whole face is divided into $d=100$ regions, each regional histogram is separately extracted, and all the extracted regional histograms are concatenated into an eLBPH, then the total length of the feature vector reaches 6,553,600 ($=65{,}536 \times 100$), which clearly is very expensive. Of course, if the number of neighbors in LBP operator is set to 8, then the total length of the feature vector is 5900 ($=59 \times 100$), shorter than the original 10,000.

Besides, in order to exhibit the properties of eLBPH as adequately and impersonally as possible, here, we briefly illustrate the sensitivity of eLBPH to the sub-block parameter. We know that the eLBPH based FR performance depends on the concatenated histogram, meanwhile, from the analysis in Section 3.2, we have grasped that

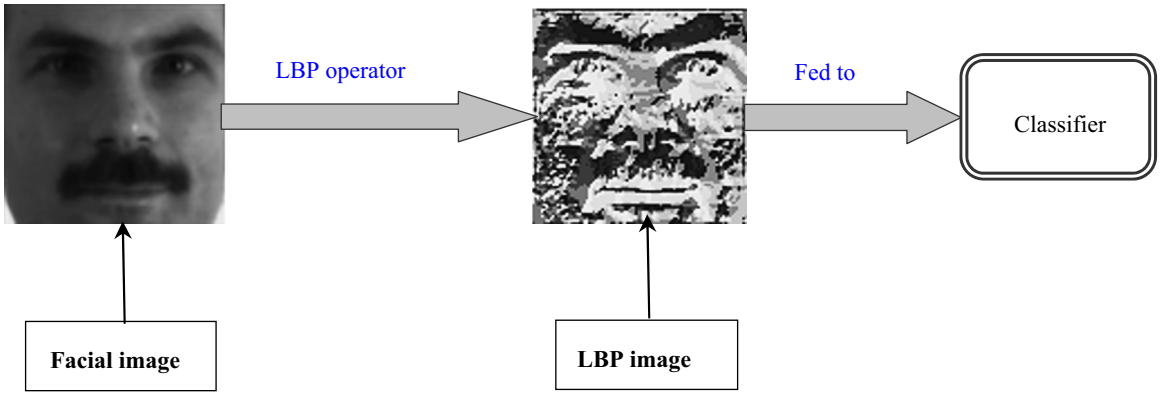

Fig. 10. The process of FR based on hLBPI.

both the stability and effectiveness of so-concatenated LBP histogram depend on the preprocessing of region division, so the eLBPH generally is sensitive to the number of so-divided regions, just as illustrated in Fig. 6(h). With the gradual increase in the number of so-divided regions, correspondingly the accuracy of FR continuously climbs up, 37.13% and 63.10% with 2 and 200 regions respectively, that is, the accuracy is improved by 25.97% at most; meanwhile, the accuracy gradually decreases with the number of so-divided regions more than 200, about 56.0% with 400 regions, dropping by 7% at most. Clearly, such results have shown that eLBPH is how sensitive to the number of so-divided regions on Yale dataset, which illuminates that the insensitivity of eLBPH to the number of so-divided regions is not true for all facial images. In fact, the eLBPH is also sensitive to the number of so-divided regions on the face datasets used in our experiments (Section 4).

Besides, it is worth noting that the region division and calculation of regional histograms in eLBPH seem somewhat arbitrary since the division possibly causes both aliasing and loss of resolution [43].

3.3. hLBPI for FR

The LBP code of the center pixel in LBP operator is calculated by Eq. (1), and the LBP codes for all pixels of an image traditionally only are used to extract the LBP histogram by Eq. (3). So, one usually only concerns their statistic histogram representation. However, the LBP **i**mage (LBPI) formed by the LBP codes,[2] as shown in Fig. 10 below, just reflects intrinsic appearances of the original image. In fact, the hLBPI has been used in [34] for face authentication or verification and modified in [32] to obtain a simplified variant. And the hLBPI feature can directly be used to FR as shown in Fig. 10 below, which is attributed to the following reasons:

From Sections 3.1–3.3, we have clearly known that the hLBPH descriptor is simple but ineffective for facial images, the eLBPH is actually sensitive to the region-division parameter, relatively complex, and absolutely losses intrinsic facial appearances, which are crucial for recognition [43], though relatively preserves spatial relations of a face. By contrast, the hLBPI of a facial image preserves both intrinsic appearances and spatial relations.

Compared to both hLBPH and eLBPH for FR, the hLBPI has own properties as follows:

(1) The extracted hLBPI feature by its definition clearly enjoys the locality robustness, the high discriminative power and the other attractive properties of LBP operator.
(2) The hLBPI quite faithfully preserves spatial relations and intrinsic appearances of facial images. In fact, the hLBPI feature for a face still is an image rather than a histogram, and vividly reflects a face, as shown in Fig. 10.
(3) The hLBPI dispenses with the preprocessing of region division and the post-processing of histogram statistic, and thus its complexity is clearly lower than those of hLBPH and eLBPH, which is illustrated by the sketch in Fig. 11.
(4) The hLBPI will not yield a longer feature vector. In fact, its dimension is slightly lower than that of input image due to the image edge is cut with the LBP operator.
(5) Like hLBPH and eLBPH, the hLBPI may also be measured by the Chi-square measure in (4), nevertheless, where B is the length of feature vector for hLBPI. So in the next section, for fairness, the Chi-square measure is adopted for all approaches based on LBP. Of course, since hLBPI is still a standard vector, naturally it can also be measured in terms of usual distance metric such as Euclidean.
(6) Though it is effective for facial images, the hLBPI is not suitable for standard texture images. The reason is that standard texture images generally have specific statistic property to a certain degree, thus, their LBP images correspondingly inherit the statistic property, as shown in Fig. 12; by contrast, the hLBPI feature has no statistic capability of histogram descriptor and thus is not an appropriate candidate, as experimentally demonstrated in Section 4.2.

4. Experiment

In this section, we evaluate and compare hLBPI, hLBPH, eLBPH and the three subspace approaches of Eigenface, Laplacianface[3] and Fisherface for FR. The adopted benchmark face datasets are FERET [44], Extended YaleB,[4] CMU PIE[5] and AR [45] with various large-variations, and the gray value per pixel is rescaled to [0 1] for increasing performances of the three subspace algorithms. In all experiments, the 1NN classifier (with Chi-square measure for hLBPI, hLBPH and eLBPH as in some references [14,15], with Euclidean one for the subspace algorithms as done in [36–38]) is

[2] *Note*: the LBP image is not a real image, and thus the corresponding experimental results are empirical ones.

[3] http://people.cs.uchicago.edu/~xiaofei/
[4] http://www.cs.uiuc.edu/homes/dengcai2
[5] http://www.cs.uiuc.edu/homes/dengcai2

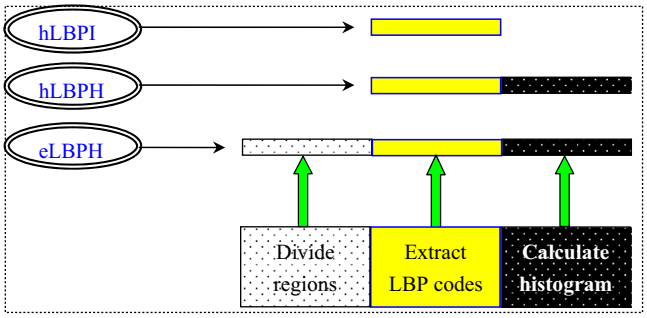

Fig. 11. Sketch of complexity for hLBPI, hLBPH and eLBPH.

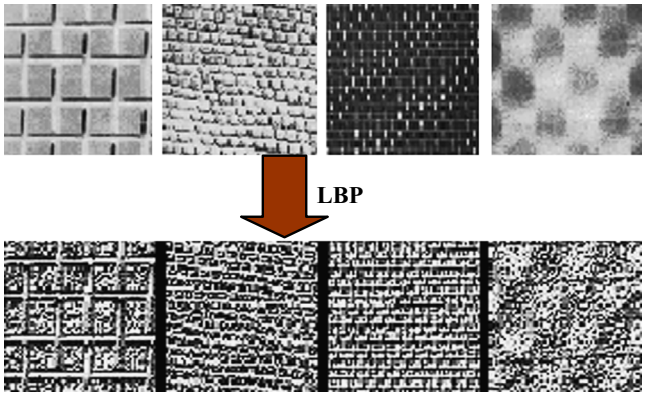

Fig. 12. LBP images of normal texture images.

adopted due to its simplicity and popularity for FR. Besides, the hLBPI is compared with hLBPH on Brodatz [39] to show hLBPI is not suitable for standard texture images.

4.1. Face recognition

4.1.1. Data description

FERET database contains 14,051 Gy-scale images of 1199 subjects with variations in pose, illumination, facial expression and age, etc. These facial images can be divided into the following five sets: ***fa*** contains 1196 gallery face images. ***fb*** contains 1195 images of subjects taken at the same time as the gallery images. The only difference is that the subjects assume a different facial expression than in the gallery image. ***fc*** contains 194 images of subjects under significantly different lighting. ***duplicate I*** contains 722 images of subjects taken between 1 min and 1031 days after the gallery image was taken. ***duplicate II*** is a subset of the duplicate I set, containing 234 images taken at least 18 months after the gallery image. Each image is resized to 60×60. Fig. 13(a) gives some sample images of the five sets.

Extended Yale B database contains 2414 front-view face images of 38 individuals. For each individual, about 64 pictures were taken under various laboratory-controlled lighting conditions. The size of each image is to 32×32. Fig. 13(b) gives some sample images of one person from this database.

CMU PIE database contains 68 individuals with 41,368 face images as a whole. The face images in PIE were captured by 13 synchronized cameras and 21 flashes, under varying pose, illumination, and expression. This used subset consists of the five near-frontal poses (C05, C07, C09, C27, C29) under different illuminations, lighting and expressions which leaves us 170 near frontal face images for each individual. The size of each image is to 32×32. Fig. 13(c) shows some sample images of one person.

AR contains over 4000 color face images for 126 persons [45]. Here, we adopt the subset of 2600 images for 100 persons (50 men and 50 women), 26 ones per person. These 26 images of each person were taken at two sessions, separated about 2 weeks, 13 images per session, with different facial expression, lighting conditions, and occlusions. Each image is resized to 60×48. Fig. 13(d) shows 26 sample images of one person.

4.1.2. Parameter setting

Here, $LBP_{P,R}$ and $LBP_{P,R}^{u2}$ (uniform pattern) respectively is adopted for hLBPI and the two features of hLBPH & eLBPH, where P, R and the pixel size of window for eLBPH are shown in Tables 1–4, for example, in Table 2, eLBPH (8×8) denotes to use the 8×8-pixel window. For an image with the size of 32×32, the number of divided regions is $(32/8) \times (32/8) = 16$. The 98% energy of PCA is kept for the three subspace algorithms. The inverse of within-class scatter matrix is replaced with the generalized-inverse in Fisherface for addressing the singularity problem. For Laplacianface, the neighbor parameter k is obtained by searching from {1,5,9} and the heat kernel width t is directly set to the mean of distances between samples, and finally the best results are reported.

4.1.3. Single image per person (SIPP)

The *single* (*training*) *image per person* (SIPP) is one challenge in FR [46]. Considering its application value, in this subsection, we specifically separately perform the experiment on this problem to evaluate the three LBP-based approaches.

We firstly adopt the FERET database to compare the three approaches, where ***fa*** is utilized as gallery set and ***fb***, ***fc***, ***dupI*** and ***dupII*** separately as probe set. Table 1 lists the accuracies of the three approaches for four probe sets, and Fig. 14 shows their accuracies for $(P, R) = (16, 2)$, where eLBPH with different window sizes. It should be noted that in our experiments, for eLBPH, we adopt neither the complex CSU Face Identification Evaluation system [46] in [14,15] nor the preprocessing in [14,15] is for making sure the achieved performance of individual approach is indeed resulted purely from the approach itself but not the complex evaluation system and the preprocessing.

Then we further use the EYaleB, CMU PIE and AR to compare the accuracies, time complexities and feature vectors of the LBP-based approaches and subspace-based approaches, the accuracies of those are listed in Table 2, the time complexities are shown in Fig. 15 and the feature vectors are shown in Fig. 16.

From Table 1 and Fig. 14, we can see that hLBPI always performs better than eLBPH except for ***fb*** with $(P, R) = (8, 1)$ while hLBPH is basically the worst one. Especially, the accuracies of hLBPI on ***fc*** for $(P, R) = (8, 1)$ and $(P, R) = (16, 2)$ are respectively 27.84% higher and 31.96% higher than the ones of eLBPH; by contrast, the accuracies of hLBPH actually only are 0%, which clearly show the suitability of hLBPH for face images with illumination. Also, it can clearly be shown by Fig. 14 that eLBPH is very sensitive to the window size on the four probe sets. The accuracies of eLBPH actually continuously increase with the change of the window size from 60×20 to 10×10, however, the maximum differences of accuracies among the five window sizes on ***fb***, ***fc***, ***dupI*** and ***dupII*** are respectively 27.78%, 12.88%, 26.18% and 12.40%. Moreover, the smallest accuracies of eLBPH for 60×20 on ***fc*** and ***dupII*** never reach so much as 1%.

From the results in Table 2 we can see that hLBPI consistently outperforms the other approaches, especially on EYaleB, the

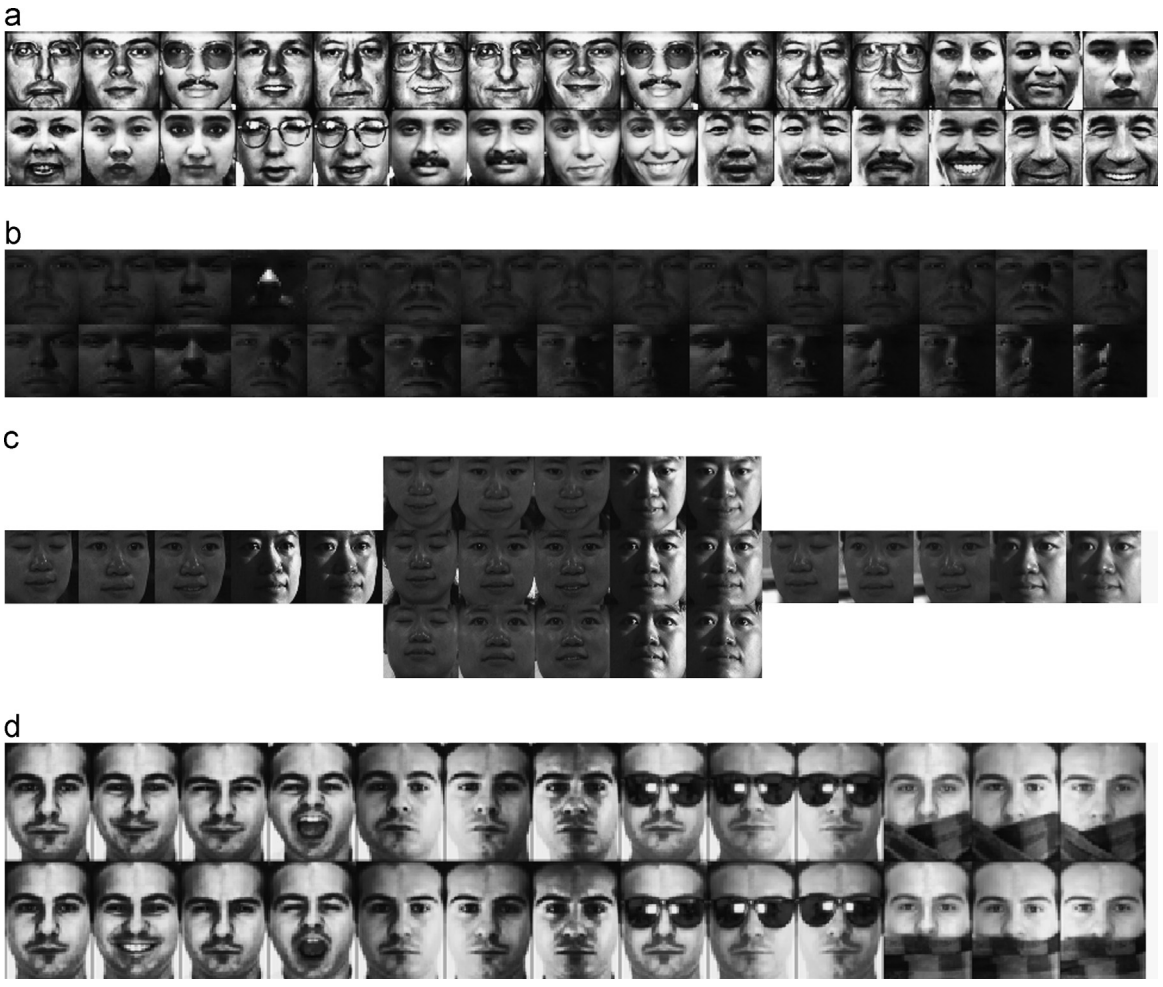

Fig. 13. Sample images of one person. (a) FERET, (b) Extended Yale B, (c) CMU PIE and (d) AR.

Table 1
Accuracy (mean) of hLBPI, eLBPH and hLBPH on FERET with ***fa***(1196) as gallery set.

Probe	(*P*, *R*)	hLBPI	hLBPH	eLBPH (60 × 20)	eLBPH (30 × 30)	eLBPH (20 × 20)	eLBPH (15 × 15)	eLBPH (10 × 10)
fb(1195)	(8, 1)	63.18	31.13	48.54	59.58	62.85	67.45	**76.32**
	(16, 2)	**70.04**	11.38	13.64	15.40	33.14	46.61	69.12
fc(194)	(8, 1)	**35.57**	0.00	0.00	1.55	3.09	4.64	7.73
	(16, 2)	**45.36**	0.00	0.52	1.03	2.58	4.12	13.40
dup I(722)	(8, 1)	**40.72**	2.91	8.17	12.33	19.25	48.62	34.35
	(16, 2)	**42.11**	1.66	1.25	2.49	4.71	10.94	22.02
dup II(234)	(8, 1)	**35.04**	0.00	0.85	2.56	6.84	9.83	13.25
	(16, 2)	**27.78**	1.28	0.00	0.43	2.56	5.13	11.11

Table 2
Accuracy (mean ± std%) of LBP and subspace based approaches on Yale B, PIE and AR. Where (16 × 16 and 8 × 8) of eLBPH are for EYaleB and CMU PIE, (33 × 24 and 22 × 12) for AR.

Data	(*P*, *R*)	Based on LBP				Based on subspace		
		hLBPI	hLBPH	eLBPH (16 × 16/33 × 24)	eLBPH (8 × 8/22 × 12)	Eigenface	Laplacianface	Fisherface
EYaleB	(8, 1)	**55.55 ± 2.12**	7.50 ± 0.68	12.30 ± 1.04	17.64 ± 1.42	10.83 ± 1.22	18.39 ± 3.07	10.83 ± 1.22
	(8, 2)	**41.51 ± 2.05**	9.03 ± 0.80	15.44 ± 0.94	19.91 ± 1.62			
PIE	(8, 1)	**29.79 ± 1.65**	9.03 ± 0.41	15.86 ± 0.86	23.71 ± 1.27	10.17 ± 0.69	15.99 ± 1.71	10.17 ± 0.69
	(8, 2)	**28.93 ± 1.45**	11.49 ± 0.35	20.48 ± 0.86	25.41 ± 1.14			
AR	(8, 1)	**31.49 ± 1.67**	10.24 ± 0.90	15.73 ± 0.97	22.90 ± 1.22	10.92 ± 0.84	14.92 ± 1.76	10.92 ± 0.84
	(16, 1)	**28.67 ± 1.45**	12.01 ± 0.94	18.72 ± 1.13	25.66 ± 1.34			

Table 3
Accuracy (mean ± std%) of LBP and subspace based approaches on EYale B.

G_m/P_n	(P, R)	Based on LBP				Based on subspace		
		hLBPI	hLBPH	eLBPH (16 × 16)	eLBPH (8 × 8)	Eigenface	Laplacianface	Fisherface
G_5/P_{33}	(8, 1)	**89.68 ± 1.36**	15.88 ± 0.96	32.55 ± 1.02	47.64 ± 0.99	29.33 ± 1.29	**63.13 ± 2.36**	***64.59 ± 1.37***
	(8, 2)	**79.49 ± 1.69**	21.96 ± 0.86	40.87 ± 1.25	52.02 ± 1.39			
G_{10}/P_{28}	(8, 1)	**96.50 ± 0.50**	21.29 ± 0.71	45.27 ± 1.02	64.88 ± 1.14	41.83 ± 1.10	***81.09 ± 1.58***	**79.01 ± 1.79**
	(8, 2)	**91.41 ± 0.74**	30.08 ± 0.86	56.49 ± 1.31	69.63 ± 1.25			
G_{20}/P_{18}	(8, 1)	**98.94 ± 0.31**	27.74 ± 0.93	57.21 ± 0.97	79.06 ± 0.97	54.85 ± 1.20	***90.97 ± 0.73***	**88.30 ± 1.04**
	(8, 2)	**97.16 ± 0.50**	39.31 ± 1.23	70.29 ± 1.43	83.98 ± 1.05			

Table 4
Accuracy (mean ± std%) of LBP and subspace based approaches on CMU PIE.

G_m/P_n	(P, R)	Based on LBP				Based on subspace		
		hLBPI	hLBPH	eLBPH (16 × 16)	eLBPH (8 × 8)	Eigenface	Laplacianface	Fisherface
G_{10}/P_{160}	(8, 1)	**79.34 ± 0.82**	29.49 ± 0.47	53.83 ± 0.57	**70.78 ± 0.68**	33.48 ± 0.46	63.03 ± 2.48	***75.49 ± 0.79***
	(8, 2)	**76.02 ± 0.86**	39.67 ± 0.68	65.70 ± 0.58	**72.85 ± 0.78**			
G_{30}/P_{140}	(8, 1)	**93.62 ± 0.31**	48.22 ± 0.49	78.55 ± 0.54	**89.99 ± 0.50**	59.55 ± 0.70	87.69 ± 0.67	***91.77 ± 0.47***
	(8, 2)	**91.81 ± 0.35**	62.71 ± 0.65	87.01 ± 0.54	**90.57 ± 0.44**			
G_{50}/P_{120}	(8, 1)	***96.00 ± 0.26***	58.44 ± 0.38	87.76 ± 0.37	**95.02 ± 0.32**	82.45 ± 0.57	93.15 ± 0.30	**96.64 ± 0.21**
	(8, 2)	***95.36 ± 0.29***	73.95 ± 0.46	87.76 ± 0.37	**95.18 ± 0.31**			

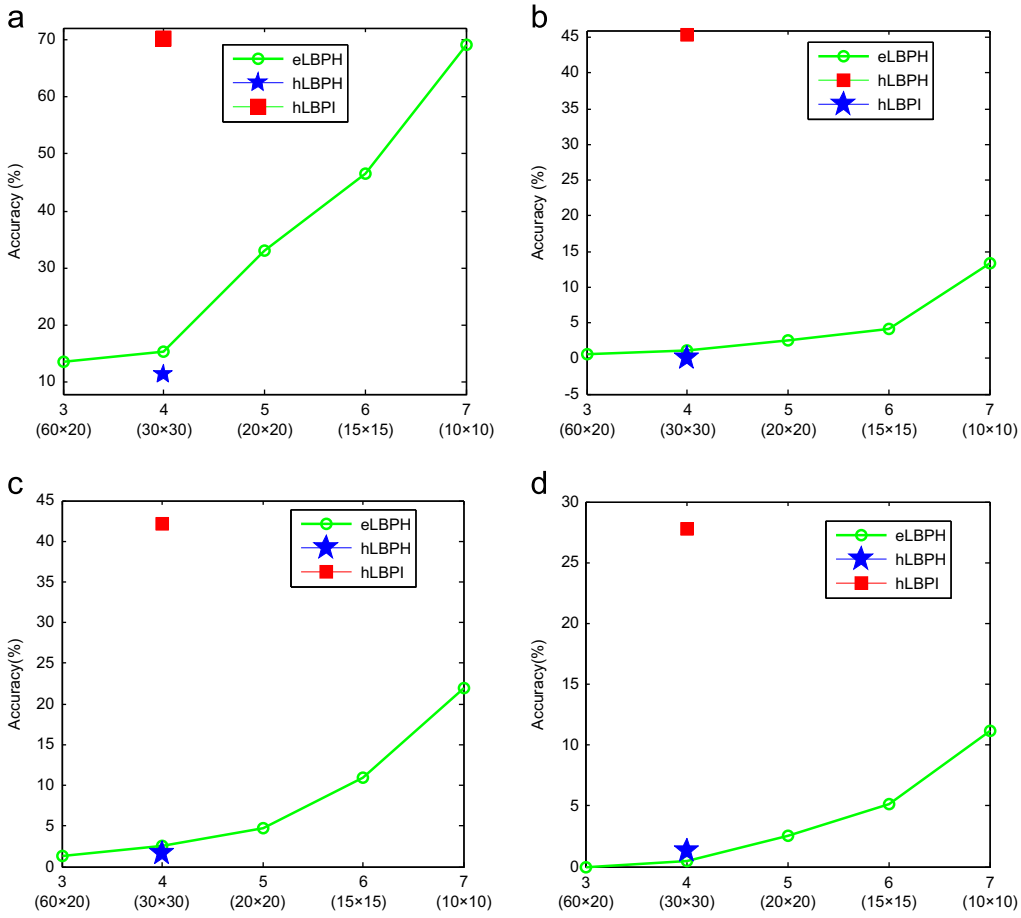

Fig. 14. Accuracy (%) of three approaches for $(P, R)=(16, 2)$, where eLBPH with different window sizes. (a) *fb*, (b) *fc*, (c) *duI* and (d) *duII*.

accuracy of hLBPI with $(P, R)=(8, 1)$ is 48.05% higher than the one of hLBPH, 43.25% and 37.91% higher than the one of eLBPH (16×16) and (8×8). In fact, for the same P and R, on EYaleB, PIE and AR, the accuracy of hLBPI is at least 21.6%, 3.5% and 3% higher than those of hLBPH and eLBPH, respectively. Meanwhile, the subspace based approaches clearly are inapplicable due to too small training samples, i.e., SIPP, as well-known.

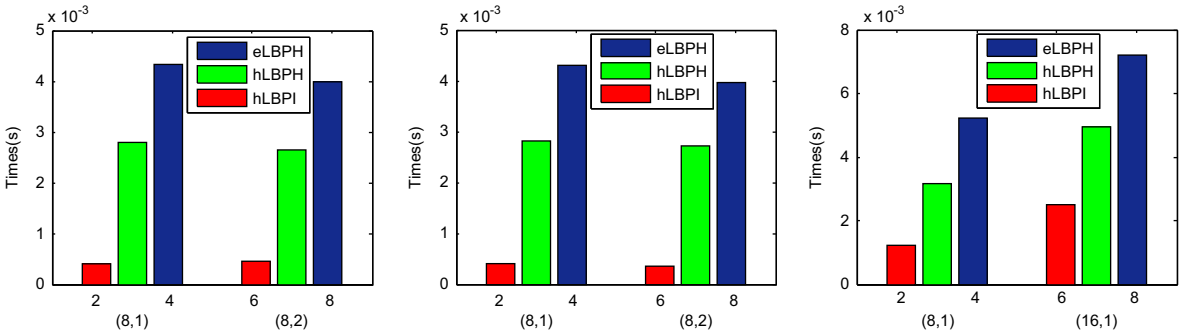

Fig. 15. Average times of eLBPH, hLBPH and hLBPI for one image with $LBP_{8,1}$, $LBP_{8,2}$ and $LBP_{16,1}$, where eLBPH, hLBPH are based on the uniform patterns (u2).

Fig. 15 shows the average times of extracting hLBPI, hLBPH and eLBPH features,[6] where the vertical axis denotes the consumed average time(s) of extracting the hLBPI, hLBPH and eLBPH features of one image on the used datasets (2414, 11,554 and 2600 images in EYaleB, PIE and AR) by a PC with Intel Quad Core Q9400 (2.67 GHz), 3 G RAM, Windows XP and Matlab 7.1 (R14). We can see that the individual times consumed by the three approaches are not much for one image. However, for all images of used datasets, their respective consumed times are very different. In fact, the times taken by hLBPI on the three datasets are all very small, concretely, less than 1 s, 5 s and 4 s with $(P, R)=(8, 1)$ on the three datasets, and about 1 s, 5 s and 7 s with $(P, R)=(8, 2)$ on EYaleB/PIE and with $(P, R)=(16, 1)$ on AR, which clearly is very promising for real applications. By contrast, the extraction of two histogram features hLBPH and eLBPH is expensive. Specifically, eLBPH consumes respectively 10.4 s, 49.7 s and 13.6 s for $(P, R)=(8, 1)$ on EYaleB/PIE and for $(P, R)=(16, 1)$ on AR, about 2-time more than hLBPI on EYaleB and PIE.

Fig. 16 shows the first 10 input images of the gallery set on AR, the corresponding hLBPH, eLBPH, hLBPI features and the first 10 base vectors of Eigen-, Laplacian- and Fisher-faces, where the length of concatenated histogram for a gallery image in eLBPH (33×24) is 236 ($=59 \times 4$). We can observe that the hLBPI vividly reflects the intrinsic appearance details of faces. For example, as shown in Fig. 16(a), the wore sunglasses of 1st, 3rd, 5th, 7th and 8th faces, the wore scarfs of 2nd and the last faces, the screaming mouth of 6th and the angry eyes of 9th faces are all vividly revealed in the corresponding hLBPI-faces in Fig. 16(b). By contrast, the histogram feature vectors of hLBPH and eLBPH are unable to reflect the appearances of input images at all. At the same time, the Eigen-, Laplacian- and Fisher-faces also reflect the appearances of face images to different degrees; however, their so-reflected effects clearly are not better than hLBPI-face, of course, which is partially attributed to too small training samples for SIPP.

4.1.4. FR with multi-gallery images per person

Each dataset is divided into different gallery/probe sets G_m/P_n. With each division of G_m/P_n for EYaleB and PIE, 30 random splits are generated and the corresponding average accuracy is reported. Meanwhile, since the facial images in AR are taken in two sessions with different expressions and occlusion variations, the four groups (G_{1-7}/P_{8-13}, G_{1-7}/P_{14-20}, G_{1-7}/P_{21-26}, G_{1-13}/P_{14-26}) are divided. Tables 3–5 respectively show the recognition performances of approaches based on LBP and subspace on EYaleB, CMU PIE and AR, where the bolded and underlined **accuracy** ranks 1st, bolded and italic ***accuracy*** 2nd and only bolded **accuracy** 3rd.

(1) From Tables 3 and 4 we can see that hLBPI always outperforms the other approaches on EYaleB and PIE except that it is slightly worse than the supervised Fisherface on PIE for G_{50}/P_{120}. Especially on EYaleB for G_{20}/P_{18}, its best accuracy reaches 98.94%; by contrast, the best result of the other approaches only is 90.97% of Laplacianface. Moreover, when the gallery images per person are relatively small, e.g., G_5/P_{33} (5 images), hLBPI far surpasses the other approaches. In fact, the hLBPI gets at least 15% and at most 74% improvements over the other approaches. Undoubtedly, hLBPI is actually promising for FR with large illumination variations.

(2) hLBPI is the best one on AR for G_{1-7}/P_{21-26} and G_{1-13}/P_{14-26} with $(P, R)=(8, 1)$, while ranks 2nd at the other cases, as shown in Table 5, whereas eLBPH is better on AR overall. Such results show that the combination of the histogram descriptor and region division strategy is a good candidate for facial images with occlusions, the reasons are as follows: the occlusion parts (sunglasses and scarf) of images are relatively uniform, for which the histogram descriptor is more suitable, and thus the corresponding concatenated histogram is less fluctuant and effective. These experimental results are consistent with the analysis above. However, the performances of eLBPH (16×16 and 8×8) on Yale B and (16×16) on PIE are unsatisfactory, which show that eLBPH yet is not alternative for facial images with large illumination variations. At the same time, the performances of eLBPH with small window (8×8 on EYaleB and PIE, 22×12 on AR) are improved over those with larger window (16×16 on EYaleB and PIE, 33×24 on AR), which demonstrates that the regional and concatenated histograms are more stable and reliable with the limited increase of so-divided regions (less window corresponding to more regions).

(3) The hLBPH is unsuccessful on the experimented face datasets, as demonstrated in Tables 3–5, which is consistent with the reports in the current works [14,15]. Specifically, its performances are always the worst on the three datasets except that it is slightly better than Eigenface on PIE for G_{30}/P_{140} with $(P, R)=(8, 2)$ and AR for G_{1-7}/P_{21-26} with $(P, R)=(16, 1)$, however, such slightly better accuracies are also unsatisfactory.

(4) As a supervised subspace approach, Fisherface shows its competence. In fact, on the three datasets, it obtains relatively excellent performance. As an unsupervised subspace approach, Laplacianface is relatively good on EYaleB, acceptable on PIE and unsatisfactory on AR. By contrast, Eigenface is the worst, in fact, it only slightly precedes hLBPI on the three datasets with several divisions of G_m/P_n.

[6] Those of subspace approaches are not shown because they need train and thus well-known relatively complex.

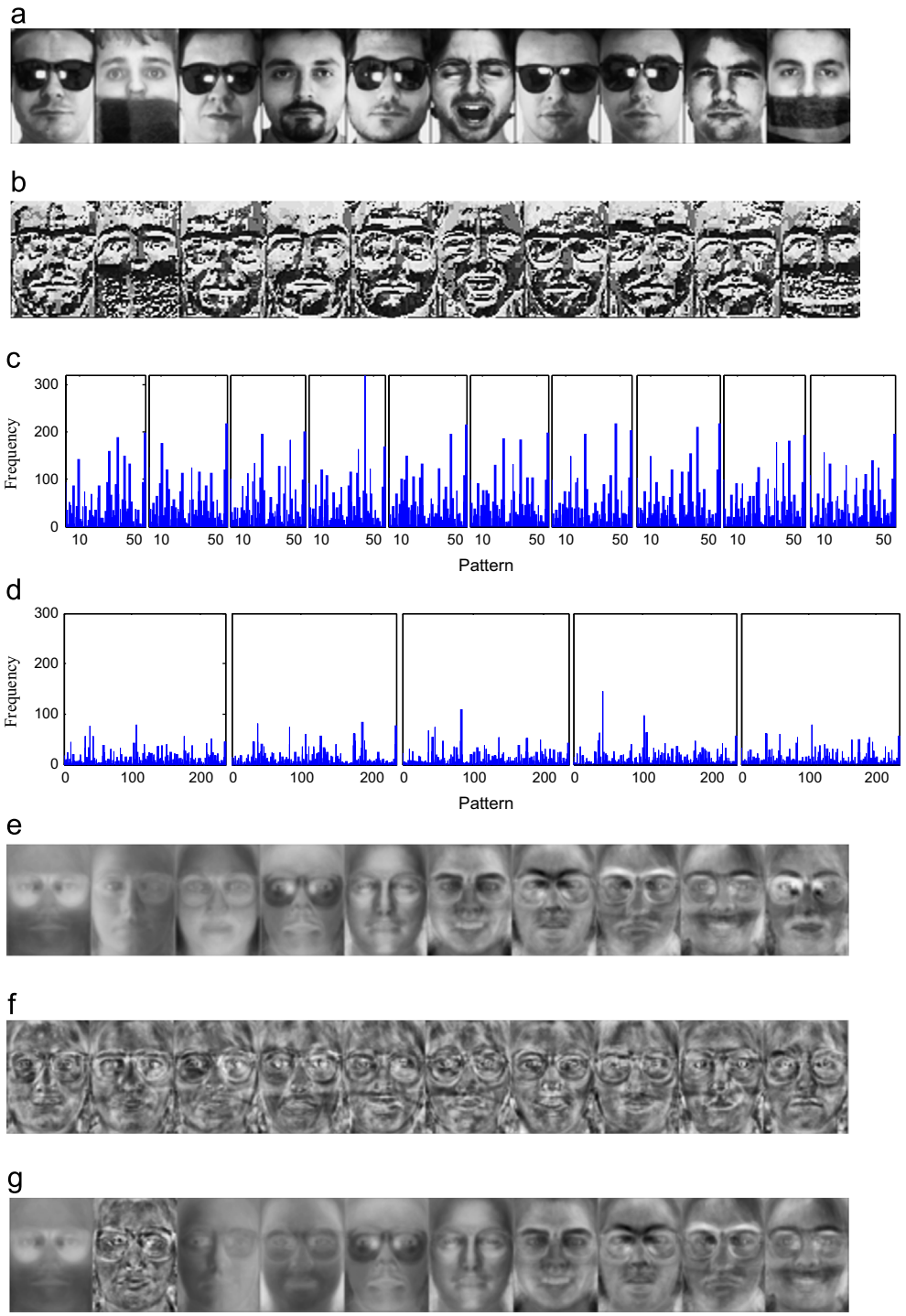

Fig. 16. The first 10 images of gallery set, the corresponding hLBPH, eLBPH (33×24) for the first 5 images, hLBPI and the first 10 base vectors of Eigen-, Laplacian- and Fisher-faces on AR. (a) The first 10 images of gallery set, (b) hLBPI for (a), (c) hLBPH for (a), (d) eLBPH for the first 5 images in (a), (e) Eigen-face, (f) Laplacian-face and (g) Fisher-face.

(5) Besides, the performance of hLBPI with $(P, R)=(8, 1)$ is better than that with $(P, R)=(8, 2)$ while the performance changes of hLBPH and eLBPH with $(P, R)=(8, 1)$ and $(8, 2)$ are on the contrary. Such results show that smaller radius is often more suitable for hLBPI since it has not the region-division locality.

4.2. Recognition for texture images

In this subsection, we perform simple texture analysis on Brodatz [39]. Our purpose is to demonstrate that hLBPI is not appropriate whereas hLBPh is a good candidate to texture images.

Brodatz contains 111 texture classes. Fig. 4(a) shows its some images. Here, each texture image is separated into 16 subimages with the size of 64×64 such that the image set consists of 1776 images of 111 classes, 16 images each class. Half images of each class are randomly chosen 20 times to comprise the gallery set and the other for the probe set, and the average result is reported.

Here, we compare hLBPI and the successful hLBPH feature with different groups of (P, R) in texture analysis. From Table 6 we can see that the accuracy of hLBPI is pathetically low, the highest one does not reach 30%, and defector consistently far worse than those

Table 5
Accuracy (%) of LBP and subspace based approaches on AR.

G_m/P_n	(P, R)	Based on LBP				Based on subspace		
		hLBPI	hLBPH	eLBPH (33×24)	eLBPH (22×12)	Eigenface	Laplacianface	Fisherface
G_{1-7}/P_{8-13}	(8, 1)	***85.67***	28.50	**61.33**	**87.00**	32.33	42.50	54.67
	(16, 1)	***88.50***	36.83	**71.33**	**91.83**			
G_{1-7}/P_{14-20}	(8, 1)	***91.43***	48.57	83.14	**93.00**	77.14	73.43	**85.14**
	(16, 1)	***91.00***	53.86	**86.72**	**93.14**			85.14
G_{1-7}/P_{21-26}	(8, 1)	**64.83**	15.17	**36.33**	***60.50***	15.50	20.50	29.67
	(16, 1)	**71.83**	17.33	**42.17**	***68.33***			
G_{1-13}/P_{14-26}	(8, 1)	**83.23**	36.31	70.15	***81.46***	61.54	59.69	**78.62**
	(16, 1)	***82.62***	41.69	74.00	**83.62**			

Table 6
Accuracies (mean $\pm$ std%) of hLBPI, hLBPH on Brodatz.

(P, R)	(16, 1)	(16, 2)	(8, 1)	(8, 2)
hLBPI	23.72 ± 0.98	26.44 ± 0.66	14.26 ± 0.78	17.23 ± 0.89
hLBPH	$\mathbf{90.45 \pm 0.75}$	$\mathbf{85.96 \pm 0.93}$	$\mathbf{89.40 \pm 0.64}$	$\mathbf{85.54 \pm 0.87}$

of hLBPH. Such results sufficiently show that hLBPI is not suitable for standard texture images.

5. Conclusion

In this paper, we do not propose a novel FR approach, but rather systematically examine and compare hLBPH, eLBPH and hLBPI, and thus discover the incapable and effective reasons of hLBPH, eLBPH and hLBPI for FR. The extensive experiments show the promising performance of hLBPI and eLBPH for FR, and the worst one of hLBPH. However, our final purpose is to provide practitioners with some guidance for reasonably selecting an appropriate approach in real tasks, so, here, we give some remarks on hLBPI, hLBPH and eLBPH as follows:

(1) The hLBPH is simple and prominent for standard texture analysis yet unsuitable for FR.
(2) The hLBPI is efficient, and is a good candidate for FR with large variations especially with illumination, yet infeasible for standard texture images.
(3) The eLBPH is relatively complex and sensitive to the region-division parameter, yet appropriate for FR with partial occlusion variations and illuminations.

Besides, the effectiveness of hLBPI for FR drives us to dedicate some further studies including

(1) utilizing the corresponding code features of existing LBP histogram variants [11,12,22,43] to obtain better FR performance,
(2) examining the impacts of some preprocessing techniques especially Gabor filter [22,33,47–49] on the hLBPI,
(3) introducing it to facial expression recognition [50,51], video recognition [52], gender classification [53], etc.

Acknowledgment

Thank the MVG group, Xiaofei He and Dengcai for providing the codes of LBP, LPP and face datasets. And thank NSFC for partial support (Grant no. 61170151), Program of Higher-Level Talents of Inner Mongolia University (No. 115118) and Sponsored by Jiangsu QingLan Project respectively.

References

[1] D. Harwood, T. Ojala, M. Pietikäinen, S. Kelman, S. Davis, Texture Classification by Center-Symmetric Auto-correlation, Using Kullback Discrimination of Distributions, Technical Report, CAR-TR-678, Computer Vision Laboratory, Center for Automation Research, University of Maryland, College Park, Maryland, 1993.
[2] T. Ojala, M. Pietikäinen, D. Harwood, A comparative study of texture measures with classification based on feature distributions, Pattern Recognition 29 (1) (1996) 51–59.
[3] T. Ojala, M. Pietikäinen, T. Mäenpää, Multiresolution gray-scale and rotation invariant texture classification with local binary patterns, IEEE Trans. Pattern Anal. Mach. Intell. 24 (7) (2002) 971–987.
[4] G. Zhao, M. Pietikainen, Dynamic texture recognition using volume local binary patterns, in: Proceedings of European Conference on Computer Vision 2006 Workshop on Dynamical Vision, 2006.
[5] T. Mäenpää, T. Ojala, M. Pietikäinen, M. Soriano, Robust texture classification by subsets of local binary patterns, in: Proceedings of 15th International Conference on Pattern Recognition, 2000, pp. 947–950.
[6] T. Mäenpää, M. Pietikäinen, T. Ojala, Texture classification by multi-predicate local binary pattern operators, in: Proceedings of 15th International Conference on Pattern Recognition, 2000, pp. 951–954.
[7] T. Ojala, T. Mäenpää, M. Pietikäinen, J. Viertola, J. Kyllönen, S. Huovinen, Outex—a new framework for empirical evaluation of texture analysis algorithms, in: Proceedings of 16th International Conference on Pattern Recognition, 2002.
[8] T. Ojala, K. Valkealahti, E. Oja, M. Pietikäinen, Texture discrimination with multi-dimensional distributions of signed gray level differences, Pattern Recognition 34 (3) (2001) 727–739.
[9] T. Mäenpää, M. Pietikäinen, Texture analysis with local binary patterns, in: C. Chen, P. Wang (Eds.), Handbook of Pattern Recognition and Computer Vision, 3rd ed.,World Scientific, Singapore, 2005, pp. 197–216.
[10] Z. Guo, L. Zhang, D. Zhang, Rotation invariant texture classification using LBP variance (LBPV) with global matching, Pattern Recognition 43 (3) (2010) 706–719.
[11] Z. Guo, L. Zhang, D. Zhang, A completed modeling of local binary pattern operator for texture classification, IEEE Trans. Image Process. 19 (6) (2010) 1657–1663.
[12] L. Nanni, A. Lumini, S. Brahnam, Local binary patterns variants as texture descriptors for medical image analysis, Artif. Intell. Med. 49 (2) (2010) 117–125.
[13] A. Fathi, A. Naghsh-Nilchi, Noise tolerant local binary pattern operator for efficient texture analysis, Pattern Recognition Letters 33 (2012) 1093–1100.
[14] L. Nanni, S. Brahnam, A. Lumini, A simple method for improving local binary patterns by considering non-uniform patterns, Pattern Recognition 45 (2012) 3844–3852.
[15] M. Pietikäinen, T. Ojala, Z. Xu, Rotation-invariant texture classification using feature distributions, Pattern Recognition 33 (1) (2000) 43–52.
[16] T. Ahonen, A. Hadid, M. Pietikäinen, Face recognition with local binary patterns, in: Proceedings of 8th European Conference on Computer Vision, 2004, pp. 469–481.
[17] T. Ahonen, A. Hadid, M. Pietikäinen, Face description with local binary patterns: application to face recognition, IEEE Trans. Pattern Anal. Mach. Intell. 28 (12) (2006) 2037–2041.
[18] D. Huang, C. Shan, M. Ardabilian, Y. Wang, L. Chen, Local binary patterns and its application to facial image analysis: a survey, IEEE Trans. Systems Man Cybern. Part C 41 (6) (2011) 765–781.
[19] A. Hadid, M. Pietikäinen, T. Ahonen, A discriminative feature space for detecting and recognizing faces, in: Proceedings of IEEE Conference on Computer Vision and Pattern Recognition, 2004, pp. 797–804.

[20] A. Hadid, The local binary pattern approach and its applications to face analysis, in: First Workshop on Image Processing Theory, Tools and Applications, 2008, pp. 1–9.
[21] A. Hadid, M. Pietikäinen, S. Li, Boosting spatio-temporal LBP patterns for face recognition from video, in: Proceedings of Asia-Pacific Workshop on Visual Information Processing, 2006, pp. 75–80.
[22] G. Zhang, X. Huang, S.Z. Li, Y Wang, X. Wu, Boosting local binary pattern (LBP)-based face recognition, in Proceedings of the Advances in Biometric Person Authentication, ser. Lecture Notes in Computer Science, 2004, pp. 179–186.
[23] S. Li, R. Chu, M. Ao, L. Zhang, R. HE, Highly accurate and fast face recognition using near infrared images, in: Proceedings of the International Conference on Advances in Biometrics, 2006, pp. 151–158.
[24] W. Zhang, S. Shan, W. Gao, X. Chen, H. Zhang, Local gabor binary pattern histogram sequence (LGBPHS): a novel non-statistical model for face representation and recognition, in: Proceedings of the Tenth IEEE International Conference on Computer Vision, 2005, pp. 786–791.
[25] C. Shan, S. Gong, P. W. McOwan, Robust facial expression recognition using local binary patterns, in: Proceedings of IEEE International Conference on Image Processing, 2005, pp. 914–917.
[26] X. Feng, M. Pietikäinen, A. Hadid, Facial expression recognition with local binary patterns and linear programming, Pattern Recognition Image Anal. 15 (2) (2005) 546–548.
[27] N. Sun, W. Zheng, C. Sun, C. Zou, L. Zhao, Gender classification based on boosting local binary pattern, in: Proceedings of 3rd International Symposium on Neural Networks, 2006, pp. 194–201.
[28] H. Jin, Q. Liu, H. Lu, X. Tong, Face detection using improved LBP under Bayesian framework, in: Proceedings of the Third International Conference on Image and Graphics, 2004, pp. 306–309.
[29] Y. Rodriguez, S. Marcel, Face authentication using adapted local binary pattern histograms, in: Proceedings of 9th European Conference on Computer Vision, 2006, pp. 321–332.
[30] J. Zhao, H. Wang, H. Ren, S. C. Kee, LBP discriminant analysis for face verification, in: Proceedings of IEEE Workshop on Face Recognition Grand Challenge Experiments, 2005, pp. 167–167.
[31] M. Sébastien, R. Yann, H. Guillaume, On the Recent Use of Local Binary Patterns for Face Authentication, Idiap-RR-34, 2006.
[32] X. Huang, S.Z. Li, Y. Wang, Shape localization based on statistical method using extended local binary pattern, in: Proceedings of the Third International Conference on Image and Graphics, 2004, pp. 184–187.
[33] L. Zhang, R. Chu, S. Xiang, S. Liao, S. Z. Li, Face detection based on multi-block lbp representation, in: Proceedings of IAPR International Conference on Biometric, vol. 4642/2007, Seoul, Korea, 2007.
[34] M. Ao, D. Yi, Z. Lei, S.Z. Li, Face recognition at a distance: system issues, in: M. Tistarelli, S.Z. Li, R. Chellappa (Eds.), Handbook of Remote Biometrics for Surveillance and Security, Springer, London, 2009.
[35] S. Xie, S. Shan, X. Chen, J. Chen, Fusing local patterns of Gabor magnitude and phase for face recognition, IEEE Trans. Image Process. 19 (5) (2010) 1349–1361.
[36] G. Heusch, Y. Rodriguez, S. Marcel, Local binary patterns as image preprocessing for face authentication, in: Proceedings of IEEE International Conference on Automatic Face and Gesture Recognition, 2006.
[37] T. Qian, R. Veldhuis, Illumination normalization based on simplified local binary patterns for a face verification system, in: Biometrics Symposium, 2007 pp. 1–6.
[38] P.N. Belhumeur, J.P. Hespanha, D.J. Kriegman, Eigenfaces vs. fisherfaces: recognition using class specific linear projection, IEEE Trans. Pattern Anal. Mach. Intell. 19 (7) (1997) 711–720.
[39] X. He, S. Yan, Y. Hu, P. Niyogi, H.J. Zhang, Face recognition using laplacianfaces, IEEE Trans. Pattern Anal. Mach. Intell. 27 (3) (2005) 328–340.
[40] A.U. Batur, M.H. Hayes, Linear subspace for illumination robust face recognition, in: Proceedings of IEEE International Conference on Computer Vision and Pattern Recognition, Hawaii, December 2001.
[41] Brodatz P., Textures: A Photographic Album for Artists and Designers [EB/OL], (2006201210) [2006210225], ⟨http://www.ux.uis.no/~tranden/brodatz/20060110.html⟩.
[42] Yale University Face Database, ⟨http://cvc.yale.edu/projects/yalefaces/yalefaces.html⟩, 2002.
[43] K.I. Laws, Texture energy measures, in: Proceedings of the Image Understanding Workshop, 1979, pp. 47–51.
[44] K.I. Laws, Textured Image Segmentation, Report 940, Image Processing Institute, University of Southern California, 1980.
[45] X. Tan, B. Triggs, Enhanced local texture feature sets for face recognition under difficult lighting conditions, IEEE Trans. Image Process. 19 (6) (2010) 1635–1650.
[46] P.J. Phillips, H. Moon, S.A. Rizvi, P.J. Rauss, The FERET evaluation methodology for face recognition algorithms, IEEE Trans. Pattern Anal. Mach. Intell. 22 (2000) 1090–1104.
[47] A. Martinez, R. Benavente, The AR Face Database, CVC Technical Report #24, June 1998.
[48] X. Tan, S. Chen, Z. Zhou, F. Zhang, Face recognition from a single image per person: a survey, Pattern Recognition 39 (9) (2006) 1725–1745.
[49] B. Zhang, S. Shan, X. Chen, W. Gao, Histogram of gabor phase patterns (hgpp): a novel object representation approach for face recognition, IEEE Trans. Image Process. 16 (1) (2007) 57–68.
[50] Y. Pang, Y. Yuan, X. Li, Gabor-based region covariance matrices for face recognition, IEEE Trans. Circuits Syst. Video Technol. 18 (7) (2008) 989–993.
[51] W. Zhang, S. Shan, X. Chen, W. Gao, Are Gabor phases really useless for face recognition? in: Proceedings of the International Conference on Pattern Recognition, 2006 pp. 606–609.
[52] T. Sha, M. Song, J. Bu, C. Chen, D. Tao, Feature level analysis for 3D facial expression recognition, Neurocomputing 74 (12) (2011) 2135–2141.
[53] G. Zhao, M. Pietikäinen, Dynamic texture recognition using Local Binary Patterns with an application to facial expressions, IEEE Trans. Pattern Anal. Mach. Intell. 27 (6) (2007) 915–928.

Bo Yang received the B.Sc. degree in Computer Applications from Jilin Normal University in 2002. She received the M.Sc. degree in Computer Applications at Anhui University of Technology in 2007. She received the Ph.D. degree in Department of Computer Science and Engineering, Nanjing University of Aeronautics & Astronautics (NUAA) in 2010. Her research interests focus on computer vision, dimensionality reduction, pattern recognition, machine learning and their applications.

Songcan Chen received the B.Sc. degree in Mathematics from Hangzhou University (now merged into Zhejiang University) in 1983. In December 1985, he completed the M.Sc. degree in Computer Applications at Shanghai Jiaotong University and then worked at Nanjing university of Aeronautics & Astronautics (NUAA) in January 1986 as an Assistant Lecturer. There he received a Ph.D. degree in Communication and Information Systems in 1997. Since 1998, as a full Professor, he has been with the College of Computer Science and Technology at NUAA. His research interests include pattern recognition, machine learning and neural computing. In these fields, he has authored or coauthored over 150 peer-reviewed scientific journal papers.